HIV-1 Tat-induced cerebrovascular toxicity is enhanced in mice with amyloid deposits

Lei Chen[1], **Jeong June Choi**[1], **Yean Jung Choi**[1], **Bernhard Hennig**[2], and **Michal Toborek**[1]

[1]Molecular Neuroscience and Vascular Biology Laboratory, Department of Neurosurgery, University of Kentucky, Lexington, Kentucky, USA

[2]College of Agriculture University of Kentucky, Lexington, Kentucky, USA

Abstract

HIV-1-infected brains are characterized by elevated depositions of amyloid beta (Aβ); however, the interactions between Aβ and HIV-1 are poorly understood. In the present study, we administered specific HIV-1 protein Tat into the cerebral vasculature of 50–52 week old double transgenic (B6C3-Tg) mice that express a chimeric mouse/human amyloid precursor protein (Mo/HuAPP695swe) and a mutant human presenilin 1 (PS1-dE9) and are characterized by increased Aβ depositions in the brain. Exposure to Tat increased permeability across cerebral capillaries, enhanced disruption of zonula occludens (ZO)-1 tight junction protein, and elevated brain expression of matrix metalloproteinase-9 (MMP-9) in B6C3-Tg mice as compared to age-matched littermate controls. These changes were associated with increased leukocyte attachment and their transcapillary migration. The majority of Tat-induced effects were attenuated by treatment with a specific Rho inhibitor, hydroxyfasudil. The results of animal experiments were reproduced in cultured brain endothelial cells exposed to Aβ and/or Tat. The present data indicate that increased brain levels of Aβ can enhance vascular toxicity and proinflammatory responses induced by HIV-1 protein Tat.

Keywords

HIV-1 infection; amyloid; HIV-1; aging; blood-brain barrier; tight junction proteins; inflammation

INTRODUCTION

The widely used combination antiretroviral therapy (cART) greatly improved the life span of HIV-1-infected patients. This therapeutic success, along with an increased number of new infections in older patients, accounts for a rapid growth of the population of older HIV-1-infected patients. Indeed, approximately 24% of HIV-1-infected individuals in the United States are 50 years of age or older (Centers for Disease Control and Prevention, 2007). It is estimated that 50% of HIV-1-infected patients will be aged 50 or more by 2015 (Myers,

Correspondence: Michal Toborek, MD. PhD, Molecular Neuroscience and Vascular Biology Laboratory, Department of Neurosurgery, University of Kentucky Medical Center, 593 Wethington Bldg., 900 S Limestone, Lexington, KY 40536, USA. michal.toborek@uky.edu, Phone numbers: 859-323-4094, Fax numbers: 859-323-2705.

DISCLOSURE STATEMENT
No actual or potential conflicts of interest.

2009). This emerging development in HIV-1 epidemic has significant consequences, because the increased age of infected patients has a detrimental effect on the progress of diseases, including the development of cognitive dysfunction and neurodegenerative diseases (Brew, et al., 2009). For example, the risk of having HIV-1-associated dementia in older patients was estimated to be more than 3 times that of the younger individuals (Valcour, et al., 2004).

While there are no unique manifestations of HIV-1 infection in older individuals, the development of specific symptom complexes, the occurrence of comorbidities, and the development of AIDS are greatly enhanced with age (Kirk and Goetz, 2009). For example, 53% older, versus 37% younger, HIV-1-infected individuals develop AIDS within 12 months of the diagnosis or die within 12 months of developing AIDS. The risk of death is estimated to be 1.5 fold as great, and the risk of developing AIDS is 1.3 fold as great, for every 10 years of age (reviewed in Kirk and Goetz, 2009). Although older patients demonstrate better adherence to therapy, they are more susceptible to the adverse effects of cART (Ettenhofer, et al., 2009), especially when the therapy includes a protease inhibitor which can affect lipid metabolism and cerebrovascular health (Hardy and Vance, 2009). Overall, older HIV-1-infected patients have higher prevalence of hypertension, hypertriglyceridemia, low body mass, and lipodystrophy than age-matched controls (Onen, et al., 2010).

Several potential mechanisms have been proposed to explain the interaction between age and the progression of HIV-1 infection in the brain. Among them, compelling evidence indicates that HIV-1 can contribute to amyloid pathology in the brain. Exposure to HIV-1 can increase amyloid beta peptide (Aβ) levels (Achim, et al., 2009) by upregulation of its formation (Aksenov, et al., 2010; Pulliam, 2009), deficient enzymatic degradation (Daily, et al., 2006; Rempel and Pulliam, 2005), or transport mechanisms in brain endothelial cells that favor Aβ accumulation in the brain (Andras, et al., 2010).

The involvement of the cerebrovascular system in HIV-1 brain infection and amyloid pathology prompted us to focus the present study on the interactions of HIV-1 specific protein Tat with Aβ at the blood-brain barrier (BBB) level. The major components of the BBB are the brain endothelial cells that interact with astrocytes and pericytes along the microvasculature. Brain endothelial cells are sealed together with tight junctions (TJs) to form the physical barrier and protect the brain against the entry of blood-borne components, including inflammatory cells (Abbott, et al., 2006). Our results demonstrate that cerebrovascular toxicity of Tat is exacerbated in transgenic mice that accumulate amyloid in the brain, resulting in increased disruption of TJ proteins.

MATERIAL AND METHODS

Animals, treatment factors, and surgical procedures

Studies were performed on aged 12 month old double transgenic mice (B6C3-Tg; Jackson Laboratory, Bar Harbor, ME) that express a chimeric mouse/human amyloid precursor protein (Mo/HuAPP695swe) and a mutant human presenilin 1 (PS1-dE9) and are characterized by Aβ deposition in the brain (Hickman, et al., 2008). B6C3-Tg mice were generated on the C57BL/6 background. Age-matched wild type littermates served as controls in all experiments. In addition, young 3 month old C57BL/6 mice were used for selected experiments.

Vessel microports were surgically placed to deliver Tat and other treatment factors into the brain vasculature of the left hemisphere via the internal carotid artery (ICA) as described earlier (Chen, et al., 2009). Tat was slowly injected as a bolus over 3 min. Specificity of Tat-

mediated effects was controlled by treatment with heat-inactivated Tat (Tat_{hi}) prepared by heating 25 µg Tat in PBS for 5 min in 100°C, followed by centrifugation of denatured protein for 30 min at 21,000 g. Endotoxins, including LPS, are not affected by these conditions. In selected experiments, mice were injected i.p. with hydroxyfasudil monohydrochloride (HF, 100 µM, a specific Rho-kinase inhibitor; Sigma, St. Louis, MO) 12 h before Tat administration.

Cranial windows were installed to observe leukocyte interactions with cerebral vessels. Under anesthesia, the left parietal bone was exposed by a midline skin incision, followed by a craniotomy (2.5 mm diameter) 2.5 mm posterior from the bregma and 2.5 mm lateral from the midline. A glass coverslip was placed and sealed with dental cement over the exposed brain tissue, which was suffused with artificial cerebrospinal fluid.

Assessments of amyloid plaques, BBB integrity, and TJ protein expression

Amyloid plaques were detected using Amyloid Stain, Congo Red staining kit (Sigma) following the manufacturer's instruction. Brain slices were rinsed, placed in Alkaline Sodium Chloride Solution for 20 min and then stained with Alkaline Congo Red Solution for 20 min. After three washes with absolute ethanol, the slices were cleared with xylene, mounted, and observed under fluorescence microscope using Texas Red filter (Ex: 560 nm, Em: 595 nm).

The BBB permeability was assessed using sodium fluorescein (2% in 100 µl PBS) as described earlier (Chen, et al., 2009). Integrity of the brain microvasculature for large molecules was visualized by using albumin solution labeled with fluorescein isothiocyanate (FITC) (Sigma) (Chen, et al., 2009). The brains were sectioned into 20 µm slices and imaged under a fluorescent microscope (excitation, 460–500 nm; emission, 510–560 nm). Immunostaining and immunoblotting of ZO-1 and claudin-5 were performed as described earlier (Pu, et al., 2005).

MMP-9 expression and gelatinase activity assays

Zymography was used to quantify MMP-9 activity in plasma as descried earlier (Huang, et al., 2009) using pre-made reagents from Invitrogen (Carlsbad, CA). Gelatinase activity was detected *in situ* in unfixed hippocampal cryostat sections using DQ-gelatin as substrate (EnzChek Protease Assay; Molecular Probes, Eugene, OR). Briefly, DQ-gelatin (100 µg/ml) was in water, applied on slices, and incubated overnight at 37°C. The slides were then fixed with 4% paraformaldehyde, sealed with cover glass, and observed using a filter with excitation at 460–500 nm and emission at 510–560 nm.

Protein expression of MMP-9 was assessed in brain tissue by Western blotting. Goat anti-MMP-9 antibody (R&D Systems, Minneapolis, MN) was used as primary antibody.

Leukocyte attachment to the brain endothelium and visualization of macrophages in brain parenchyma

Mice were injected with 50 µl rhodamine 6-G (Rho6-G) chloride in PBS solution (1 µg/100 µl). Rho6-G is a highly cell permeable dye and when administered i.v. is readily sequestered by active mitochondria of leukocytes present in the blood stream. Erythrocytes do not contain mitochondria and, therefore, do not take up the dye. Rho6-G was allowed to circulate for 15 min and live images of stained leukocytes were visualized and recorded using a high sensitivity CCD camera mounted on a confocal microscope with a filter for Tex-Red. Images were recorded at 5 frames/s for 60 seconds.

The presence of activated macrophages in brain parenchyma in relation to the cerebral vessels was detected by immunofluorescence. The brain slices were stained with rabbit anti-Factor VIII (1:1000 dilution, Invitrogen), followed by Tex-Red labeled secondary antibody to detect the cerebral vessels. The slides were then counter-stained with anti-F4/80 antibody labeled with FITC (1:500, Abcam, Cambridge, MA) to detect macrophages.

Cultures of human brain microvascular endothelial cells and *in vitro* treatment factors

Human brain microvascular endothelial cell line (HCMEC/D3 cells) (Weksler, et al., 2005) was cultured as described earlier (Andras, et al., 2010; Zhong, et al., 2008). Aβ(1–40) was purchased from Anaspec (San Jose, CA) and dissolved in sterile ultra pure water. Freshly solubilized Aβ without preaggregation was used in the final concentration of 1 μM. HIV-Tat(1–72) was produced as described by Ma and Nath (1997) and used at the final concentration of 100 nM. The final concentrations of Aβ and Tat were based on dose-response experiments reported earlier by our group (Andras, et al., 2008; Zhong, et al., 2008). In selected experiments, HCMEC/D3 cells were pre-treated with HF (100 μM; Sigma) 12 h prior to Tat and/or Aβ treatment.

Integrity of HCMEC/D3 monolayers, leukocyte attachment, and transendothelial migration

Endothelial permeability was assessed using FITC-dextran 20 (MW 20 kDa; 0.5 mg/ml, Sigma) as described earlier (Andras, et al., 2005). Expression of TJ proteins ZO-1 and claudin-5 was determined as described by Andras, et al. (2005). The adhesion of THP-1 cells (a human acute monocytic leukemia cell line) to HCMEC/D3 cells was assessed according to the method of Braut-Boucher, et al. (1995).

For transendothelial migration measurements, HCMEC/D3 cells were cultured on the Transwell inserts until reaching confluency. The cells were pre-treated with HF or vehicle for 12 h, washed, and placed in the wells containing serum free endothelial basal medium with added CCL-2 (50 ng/ml) as chemoattractant. Then, Tat and/or Aβ was added in the concentrations of 100 nM and/or 1 μM, respectively. THP-1 cells were stained with calcein AM (5 μM, for 15 min) and added in the amount of 2.5×10^5 on top of HCMEC/D3 monolayers for 2 h at 37°C. Thereafter, 400 μl aliquots from the lower compartments that contained migrated leukocytes were transferred to new 12-well plates and lysed in 150 μl 4% TritonX-100. Florescence was measured as a marker of cell migration at 485 nm excitation and 530 nm emission wavelengths.

Statistical analysis

One- or two-way ANOVA, followed by Newman-Keuls Multiple Comparison Test, was used to compare mean responses among the treatments. Statistical probability of $p < 0.05$ was considered significant.

RESULTS

Tat-induced disruption of the BBB integrity is enhanced in aged B6C3-Tg mice

Alterations of brain microvasculature permeability were studied using our new delivery technique, which allows Tat administration directly into the cerebral vessels, mimicking the pathological setting (Chen, et al., 2009). In order to establish the time and dose-dependent effects, the initial studies were performed using young (3 month old) wild type C57BL/6 mice. Tat at the dose of 5, 25, or 50 μg was administered for 3, 24, or 2×12 h, with mannitol being used as a positive control (Figure 1A). BBB integrity was assessed using sodium fluorescein as a low molecular weight tracer. Among different doses of Tat used at a 3 h exposure time, treatment with 25 and 50 μg Tat resulted in elevated BBB permeability. However, disruption of the BBB integrity was more pronounced after a 24 h exposure time

to Tat. Therefore, we used a 24 h exposure time to determine the effects of Tat on the BBB permeability in aged (12 month old) wild type and B6C3-Tg mice. Injection with Tat_{hi} did not affect BBB integrity.

Exposure to 50 μg Tat induced similar changes in the BBB permeability in young (3 month old) and aged (12 month old) C57BL/6 mice (Figure 1B). However, Tat-induced effects were markedly potentiated in aged B6C3-Tg mice as compared to either young or age-matched wild type controls. Inhibition of RhoA inhibitor by HF (100 μM) effectively protected against Tat-induced permeability changes.

Tat-induced leakage of cerebral microvessels was visualized by cardiac perfusion of FITC-labeled albumin 24 h post Tat treatment (Figure 1C). Intact BBB is impermeable to albumin; thus, FITC-albumin staining was restricted to cerebral vessels of vehicle-injected animals. In contrast, Tat-injected hemispheres showed a diffuse distribution of fluorescence in the brain parenchyma, indicating transcapillary leakage of FITC-albumin (Figure 1C, arrows). These changes appeared to be most advanced in aged B6C3-Tg mice.

In order to visualize distribution of Aβ in relationship to cerebral vessels, aged (12 month old) B6C3-Tg mice were perfused with FITC-albumin, followed by staining of the brain sections with Congo Red to detect amyloid. As indicated in Figure 1D, advanced amyloid plaques are surrounded by a diffused microvessel network with substantial capillary leakage, indicating compromised BBB integrity.

Exposure to Tat alters TJ protein expression in young and older mice

The integrity of TJs of brain microvessels regulates the BBB permeability. In young wild type mice, Tat administration (25 μg for 24 h) resulted in a significant decrease in ZO-1 and claudin-5 expression (Figures 2A and B, respectively). Exposure to Tat (but not Tat_{hi}) also markedly decreased the levels of TJ protein expression in aged mice; however, these effects were similar to those in young mice. Inhibition of RhoA by pretreatment of mice with HF was highly effective in protecting against Tat-induced disruption of TJ proteins in both young and aged wild type mice. In aged B6C3-Tg mice, HF was ineffective in Tat-induced downregulation of ZO-1 levels; however, it prevented Tat-mediated alteration of claudin-5 expression (Figures 2A and B, respectively).

Expression of ZO-1 and claudin-5 proteins was also visualized in cerebral vessels by immunostaining. TJ proteins showed continuous and linear staining along the vessels in control mice. In contrast, Tat administration disrupted this linear distribution and induced a fragmented and discontinuous immunoreactivity pattern (Figures 2A and 2B, right panels). These changes were similar in all types of mice evaluated in this study.

Tat-induced MMP-9 expression is potentiated in aged mice

Activity of MMPs, and in particular MMP-9, is another important element that regulates the integrity of the BBB and permeability across the brain endothelium. Plasma MMP-9 activity increased in young mice injected with Tat by ~50%. This effect was much more pronounced in aged wild type and B6C3-Tg mice, in which administration of Tat resulted in an elevation of MMP-9 activity by ~130%. Pretreatment with HF decreased Tat-induced plasma MMP-9 activity to control levels both in aged wild type and B6C3-Tg mice (Figure 3A). The effects of Tat_{hi} on plasma MMP-9 activity were minimal and did not reach statistical significance.

The influence of Tat on MMP-9 expression and gelatinase activity were also evaluated by Western blotting (Figure 3B) and *in situ* zymography (Figure 3C) in the brains of aged B6C3-Tg mice and age-matched wild type controls. B6C3-Tg mice exhibited higher baseline expression of MMP-9 as compared to wild type controls. Tat administration

markedly increased MMP-9 protein levels in aged wild type controls but not in B6C3-Tg mice as indicated by Western blotting (Figure 3B). However, Tat injection increased gelatinase activity (originated from MMP-9 or MMP-2) in hippocampal sections of both aged B6C3-Tg and corresponding wild type mice as visualized by *in situ* zymography (Figure 3C).

Exposure to Tat induces leukocyte aggregation and attachment to the brain endothelium

Disruption of the BBB integrity and alterations of MMP activity are frequently associated with increased transcapillary migration of leukocytes into the brain parenchyma. Visualization of leukocyte attachment was performed in real time via cranial window. A 3 h exposure to Tat induced aggregation of leukocytes in brain vessels that resulted in the formation of temporary cell clusters apparently attached to the endothelium of brain vessels (Figure 4A). Importantly, pretreatment of animals with HF protected against these effect. Exposure to Tat_{hi} did not demonstrate visible impact on leukocyte attachment or recruitment.

We also evaluated the interactions of monocytes with the capillary endothelium by staining the brain sections for the presence of the F4/80 antigen (a marker of monocytes/macrophages) and factor VIII (a marker of endothelial cells) (Figure 4B). Brains of aged wild-type controls showed a minimal presence of F4/80-positive cells interacting with the endothelium; however, Tat treatment markedly increased the presence of these cells in brain parenchyma (Figure 4B, open arrows). In contrast to wild-type mice, aged B6C3-Tg mice were characterized by an enhanced colocalization of F4/80-positive cells with brain endothelium (Figure 4B, closed arrows). Injection with Tat to aged B6C3-Tg mice further increased these interactions (Figure 4B, closed arrows) without any apparent increase in the presence of F4/80-positive cells in brain parenchyma.

Aβ potentiates Tat-induced toxicity in brain endothelial cells

We hypothesized that elevated brain levels of Aβ in B6C3-Tg mice contribute to increased cerebrovascular toxicity of Tat as compared to age-matched littermate controls. To address this hypothesis, cultured brain endothelial cells (HCMEC/D3 cells) were exposed to Tat in the presence or absence of Aβ and evaluated for monolayer integrity and TJ protein expression (Figure 5). Exposure to Aβ induced a relatively mild increase in permeability across the HCMEC/D3 monolayers, while these changes were more pronounced in cells treated with Tat (100 nM) (Figure 5A). The most pronounced disruption of HCMEC/D3 integrity was observed in cells exposed to both Aβ and Tat. Interestingly, inhibition of the RhoA signaling by HF significantly protected against Tat and Aβ-induced alterations of endothelial permeability, mimicking the *in vivo* results obtained in aged B6C3-Tg mice.

In studies on TJ protein expression, treatment with Aβ or Tat alone induced a significant decrease in ZO-1 and claudin-5 protein levels (Figure 5B). The most pronounced changes in claudin-5 levels were observed in cultures exposed to both Aβ and Tat. Pretreatment of HCMEC/D3 cells with HF did not alter the effects of Aβ and/or Tat on ZO-1; however, it protected against alterations of claudin-5 levels, indicating specific mechanisms leading to alterations of individual TJ protein expression.

Our experiments also involved evaluation of the effects of Aβ and Tat on adhesion of monocytic THP-1 cells to the monolayers of brain endothelial cells (Figure 5C). While treatment with Aβ did not affect adhesion of THP-1 cells, exposure to Tat (but not to Tat_{hi}) markedly stimulated this effect. A combined treatment with Tat plus Aβ exerted similar effects as Tat alone. Inhibition of RhoA kinase by HF was effective in protection against Tat-mediated elevated adhesion of THP-1 cells, mimicking the *in vivo* effects. These effects

were also reflected in studies on the influence of Tat and/or Aβ on transendothelial migration of THP-1 cells (Figure 5D). In cell adhesion and transmigration assays, only HCMEC/D3 cultures, and not THP-1 cells, were pre-treated with HF to ensure specific endothelial cell responses.

DISCUSSION

The brain has been recognized as an immune privilege organ protected from the blood-borne pathogenic factors by the BBB. The disrupted BBB results in dysfunctional metabolite and exchange function, leakage of blood components into the brain parenchyma, and migration of circulatory monocytes into the brain (Abbott, et al., 2006). Integrity of the BBB is also markedly affected in aging (Finch, 2005; Kalaria, 2009) and HIV-1 infection (Banks, et al., 2006). During HIV-1 infection, migrating monocytes carry virus into the brain to create HIV-1 reservoirs in the CNS (Nottet, et al., 1996). Comorbidities, such as aging and brain accumulation of Aβ, may additionally contribute to the alterations of the BBB integrity and facilitate disease processes resulting in cell death and cognitive impairment (Farrall and Wardlaw, 2009; Mattson and Magnus, 2006; Yankner, et al., 2008).

While Aβ deposits in the brain and Aβ plasma levels achieve high levels in Alzheimer's disease and are directly linked to the development of this disease, even normal aging is associated with increased Aβ accumulation in the CNS. In addition, HIV-1-infected brains are characterized by increased levels of Aβ (Achim, et al., 2009; Rempel and Pulliam, 2005). Therefore, to model the interaction between Aβ and HIV-1 in the cerebral vessels, the present study was based on administration of Tat into the cerebral vasculature of 12 month old B6C3-Tg mice which are characterized by substantial accumulation of Aβ in the brain.

HIV-1 Tat protein and Aβ peptide can induce several toxic effects in the cerebral vasculature, including induction of oxidative stress, alterations of TJ integrity, and activation of MMPs (Avraham, et al., 2004; Farkas and Luiten, 2001; Toborek, et al., 2003). Circulatory Aβ has been shown to affect the integrity of cerebral vessels and induce BBB dysfunction. In addition, Aβ is a proinflammatory agent that can upregulate numerous chemokines and cytokines, influencing the transmigration of cells or the integrity of the BBB (Zlokovic, 2008). Aβ can cross the BBB using a receptor for advanced glycation end products (RAGE) as a transport system (Deane, et al., 2003). Elevated brain levels of Aβ induce cerebral angiopathy and the BBB dysfunction (Thal, et al., 2008; Zipfel, et al., 2009). Moreover, exposure to HIV-1 and Tat can also induce a plethora of vascular changes that may result in alterations of the BBB integrity (Weis, et al., 1996). The BBB changes described before a common use of antiretroviral therapy include an increase in the diameter of cortical vessels, surface area density, and volume fractions. These changes were associated with thinning of the basal lamina, a decreased immunoreactivity of collagen IV, and loss of glycoproteins in the membrane of endothelial cells (Weis, et al., 1996).

Due to overlapping effects of Tat and Aβ on cerebral vasculature, we hypothesized that these factors can cross-influence their toxic effects and thus contribute to the breakdown of BBB integrity. The results of the present study revealed that younger and aged wild type mice have similar baseline levels of BBB integrity as the aged mice with increased Aβ deposits in the brain. Nevertheless, aged B6C3-Tg mice were more susceptible to the cerebrovascular toxicity of Tat, suggesting that deposits of Aβ in the brain make these mice more prone to BBB breakdown. These results are in line with clinical data that indicate increased permeability across the BBB with increasing age. BBB permeability is also increased in patients with either vascular or Alzheimer's dementia as compared with age-matched controls (Farrall and Wardlaw, 2009).

An increase in MMP-9 expression and activity is one of the common changes in neurodegenerative CNS disorders associated with the BBB breakdown (Yong, et al., 2001). Indeed, MMP-9 levels are elevated both in Alzheimer's disease (Rosenberg, 2009) and in CNS infection by HIV-1 (Conant, et al., 1999). In our recent study, we reported that MMP-9 expression and activity are increased in HIV-1-exposed brain endothelial cells (Huang, et al., 2009). The role of MMP-9 in disruption of the BBB integrity was supported by the findings that inhibition of MMP-9 can protect against barrier dysfunction of the BBB and reduce leukocyte attachment to the brain endothelium (Chrissobolis and Sobey, 2006; Slotta, et al., 2006). Consistent with these reports, we observed in the present study that MMP-9 activity was increased in plasma in response to Tat treatment in young and, especially, in aged mice. In addition, baseline activity of MMP-9 was elevated in the brains of B6C3-Tg mice as compared to age-matched controls.

The role of Rho kinase in the cerebrovascular system has been recently recognized (Chrissobolis and Sobey, 2006; Mueller, et al., 2005; Persidsky, et al., 2006; Zhong, et al., 2009). The Rho signaling plays a critical role in maintaining the integrity of the BBB by the regulation of the actin cytoskeleton, MMP induction, and modulation of TJ integrity (Wennerberg, et al., 2005). In fact, RhoA and Rac1 were shown to regulate occludin phosphorylation, stress fiber formation, and endothelial permeability (Hirase, et al., 2001; Persidsky, et al., 2006). Our recent results also indicated that Tat-induced toxic effects on brain endothelial cells are mediated, at least in part, by the Rho pathway and are linked to lipid raft-associated processes (Zhong, et al., 2009; Zhong, et al., 2008). Therefore, we employed a Rho inhibitor, hydroxyfasudil, to attenuate Aβ and Tat-induced cerebrovascular toxicity. Treatment with HF was highly effective in protecting against Aβ and/or Tat-induced alterations of endothelial integrity, MMP-9 upregulation, and leukocyte attachment. These results are in agreement with the reports that Rho signaling can regulate TJ protein expression by influencing tyrosine kinase activity, which then affects TJ protein phosphorylation (Persidsky, et al., 2006; Ramirez, et al., 2008). In addition, Rho kinase can regulate the BBB permeability via its effects on the cytoskeleton. For example, stimulation of the RhoA/ROCK signaling sequences to the phosphorylated myosin-binding subunit of myosin light chain (MLC) with the subsequent cross-linking of F-actin into stress fibers (Persidsky, et al., 2006). To support the role of Rho kinase in regulation of TJ protein expression, our study indicated that treatment with HF attenuated alterations of claudin-5 protein levels induced by co-treatment with Aβ and Tat in hCMEC/D3 cells. On the other hand, treatment with HF was ineffective in protection against Aβ plus Tat-induced changes in ZO-1 levels, illustrating differential regulation of expression of specific TJ proteins. Indeed, claudin-5 is a transmembrane protein, while ZO-1 links transmembrane TJ proteins to actin cytoskeleton.

The ultimate outcome of the disrupted BBB is increased leukocyte migration into the brain parenchyma and the development of neuroinflammation. During HIV-1 infection, these processes are believed to contribute to virus entry into the brain via infected leukocytes and propagation of inflammatory responses. In the present study, Tat injection into the cerebral vessels markedly increased interactions of leukocytes with cerebral vessels; the effects that were consistent with earlier reports based on injections of Tat into the brain parenchyma (Pu, et al., 2003). Several mechanisms can be responsible for these effects (Austin and Combs, 2010), including stimulation of CCL-2 and adhesion molecules (Eugenin, et al., 2006; Toborek, et al., 2003). CCL-2 is a potent chemokine involved in leukocyte aggregation and transendothelial migration, which emerged as a critical proinflammatory mediator in HIV-1 infection. Increased levels of CCL-2 in the spinal fluid are commonly found in HIV-1 patients with CNS disease (Cinque, et al., 1998). Adhesion molecules, such as intercellular adhesion molecule-1 (ICAM-1) and vascular cell adhesion molecule-1 (VCAM-1) are directly involved in leukocyte attachment to the vascular endothelium.

Mechanistically, Tat is known to activate transcription factors, such as nuclear factor-κB (NF-κB), which controls induction of expression of CCL-2 and adhesion molecules and thus influences leukocyte attachment and their transendothelial migration. This proposed mechanism is supported by the observations that pretreatment with HF protected against Tat-induced leukocyte attachment both *in vivo* and *in vitro*. Indeed, the Rho signaling was demonstrated to be involved in activation of NF-κB in response to several different stimuli (Shimada and Rajagopalan, 2010).

In summary, our findings indicate that Aβ deposits in transgenic animals or treatment of brain endothelial cells with exogenous Aβ can increase cerebrovascular toxicity of HIV-1 protein Tat. This effect was evident in the studies on the BBB permeability and alterations of TJ expression. Treatment with HF attenuated several aspects of Aβ and Tat cerebrovascular toxicity, indicating the importance of the Rho signaling pathway in disruption of BBB integrity.

Acknowledgments

References

Abbott NJ, Ronnback L, Hansson E. Astrocyte-endothelial interactions at the blood-brain barrier. Nat Rev Neurosci. 2006; 7:41–53. [PubMed: 16371949]

Achim CL, Adame A, Dumaop W, Everall IP, Masliah E. Increased accumulation of intraneuronal amyloid beta in HIV-infected patients. J Neuroimmune Pharmacol. 2009; 4:190–199. [PubMed: 19288297]

Aksenov MY, Aksenova MV, Mactutus CF, Booze RM. HIV-1 protein-mediated amyloidogenesis in rat hippocampal cell cultures. Neurosci Lett. 2010; 475:174–178. [PubMed: 20363291]

Andras IE, Eum SY, Huang W, Zhong Y, Hennig B, Toborek M. HIV-1-induced amyloid beta accumulation in brain endothelial cells is attenuated by simvastatin. Mol Cell Neurosci. 2010; 43:232–243. [PubMed: 19944163]

Andras IE, Pu H, Tian J, Deli MA, Nath A, Hennig B, Toborek M. Signaling mechanisms of HIV-1 Tat-induced alterations of claudin-5 expression in brain endothelial cells. J Cereb Blood Flow Metab. 2005; 25:1159–1170. [PubMed: 15815581]

Andras IE, Rha G, Huang W, Eum S, Couraud PO, Romero IA, Hennig B, Toborek M. Simvastatin protects against amyloid beta and HIV-1 Tat-induced promoter activities of inflammatory genes in brain endothelial cells. Mol Pharmacol. 2008; 73:1424–1433. [PubMed: 18276775]

Austin SA, Combs CK. Amyloid precursor protein mediates monocyte adhesion in AD tissue and apoE(−)/(−) mice. Neurobiol Aging. 2010; 31:1854–1866. [PubMed: 19058878]

Avraham HK, Jiang S, Lee TH, Prakash O, Avraham S. HIV-1 Tat-mediated effects on focal adhesion assembly and permeability in brain microvascular endothelial cells. J Immunol. 2004; 173:6228–6233. [PubMed: 15528360]

Banks WA, Ercal N, Price TO. The blood-brain barrier in neuroAIDS. Curr HIV Res. 2006; 4:259–66. [PubMed: 16842079]

Braut-Boucher F, Pichon J, Rat P, Adolphe M, Aubery M, Font J. A non-isotopic, highly sensitive, fluorimetric, cell-cell adhesion microplate assay using calcein AM-labeled lymphocytes. J Immunol Methods. 1995; 178:41–51. [PubMed: 7829864]

Brew BJ, Crowe SM, Landay A, Cysique LA, Guillemin G. Neurodegeneration and ageing in the HAART era. J Neuroimmune Pharmacol. 2009; 4:163–174. [PubMed: 19067177]

Centers for Disease Control and Prevention. HIV/AIDS Surveillance Report 2005. Atlanta: U.S. Department of Health and Human Services, Centers for Disease Control and Prevention; 2007.

Chen L, Swartz KR, Toborek M. Vessel microport technique for applications in cerebrovascular research. J Neurosci Res. 2009; 87:1718–1727. [PubMed: 19115415]

Chrissobolis S, Sobey CG. Recent evidence for an involvement of rho-kinase in cerebral vascular disease. Stroke. 2006; 37:2174–2180. [PubMed: 16809566]

Cinque P, Vago L, Mengozzi M, Torri V, Ceresa D, Vicenzi E, Transidico P, Vagani A, Sozzani S, Mantovani A, Lazzarin A, Poli G. Elevated cerebrospinal fluid levels of monocyte chemotactic protein-1 correlate with HIV-1 encephalitis and local viral replication. AIDS. 1998; 12:1327–1332. [PubMed: 9708412]

Conant K, McArthur JC, Griffin DE, Sjulson L, Wahl LM, Irani DN. Cerebrospinal fluid levels of MMP-2, 7, and 9 are elevated in association with human immunodeficiency virus dementia. Ann Neurol. 1999; 46:391–398. [PubMed: 10482270]

Daily A, Nath A, Hersh LB. Tat peptides inhibit neprilysin. J Neurovirol. 2006; 12:153–160. [PubMed: 16877296]

Deane R, Du Yan S, Submamaryan RK, LaRue B, Jovanovic S, Hogg E, Welch D, Manness L, Lin C, Yu J, Zhu H, Ghiso J, Frangione B, Stern A, Schmidt AM, Armstrong DL, Arnold B, Liliensiek B, Nawroth P, Hofman F, Kindy M, Stern D, Zlokovic B. RAGE mediates amyloid-beta peptide transport across the blood-brain barrier and accumulation in brain. Nat Med. 2003; 9:907–913. [PubMed: 12808450]

Ettenhofer ML, Hinkin CH, Castellon SA, Durvasula R, Ullman J, Lam M, Myers H, Wright MJ, Foley J. Aging, neurocognition, and medication adherence in HIV infection. Am J Geriatr Psychiatry. 2009; 17:281–290. [PubMed: 19307857]

Eugenin EA, Osiecki K, Lopez L, Goldstein H, Calderon TM, Berman JW. CCL2/monocyte chemoattractant protein-1 mediates enhanced transmigration of human immunodeficiency virus (HIV)-infected leukocytes across the blood-brain barrier: a potential mechanism of HIV-CNS invasion and NeuroAIDS. J Neurosci. 2006; 26:1098–1106. [PubMed: 16436595]

Farkas E, Luiten PG. Cerebral microvascular pathology in aging and Alzheimer's disease. Prog Neurobiol. 2001; 64:575–611. [PubMed: 11311463]

Farrall AJ, Wardlaw JM. Blood-brain barrier: ageing and microvascular disease-systematic review and meta-analysis. Neurobiol Aging. 2009; 30:337–352. [PubMed: 17869382]

Finch CE. Developmental origins of aging in brain and blood vessels: an overview. Neurobiol Aging. 2005; 26:281–291. [PubMed: 15639305]

Hardy DJ, Vance DE. The neuropsychology of HIV/AIDS in older adults. Neuropsychol Rev. 2009; 19:263–272. [PubMed: 19247836]

Hickman SE, Allison EK, El Khoury J. Microglial dysfunction and defective beta-amyloid clearance pathways in aging Alzheimer's disease mice. J Neurosci. 2008; 28:8354–60. [PubMed: 18701698]

Hirase T, Kawashima S, Wong EY, Ueyama T, Rikitake Y, Tsukita S, Yokoyama M, Staddon JM. Regulation of tight junction permeability and occludin phosphorylation by Rhoa-p160ROCK-dependent and -independent mechanisms. J Biol Chem. 2001; 276:10423–10431. [PubMed: 11139571]

Huang W, Eum SY, Andras IE, Hennig B, Toborek M. PPARalpha and PPARgamma attenuate HIV-induced dysregulation of tight junction proteins by modulations of matrix metalloproteinase and proteasome activities. FASEB J. 2009; 23:1596–1606. [PubMed: 19141539]

Kalaria RN. Linking cerebrovascular defense mechanisms in brain ageing and Alzheimer's disease. Neurobiol Aging. 2009; 30:1512–1514. [PubMed: 18187235]

Kirk JB, Goetz MB. Human immunodeficiency virus in an aging population, a complication of success. J Am Geriatr Soc. 2009; 57:2129–2138. [PubMed: 19793157]

Ma M, Nath A. Molecular determinants for cellular uptake of Tat protein of human immunodeficiency virus type 1 in brain cells. J Virol. 1997; 71:2495–2499. [PubMed: 9032389]

Mattson MP, Magnus T. Ageing and neuronal vulnerability. Nat Rev Neurosci. 2006; 7:278–294. [PubMed: 16552414]

Mueller BK, Mack H, Teusch N. Rho kinase, a promising drug target for neurological disorders. Nat Rev Drug Discov. 2005; 4:387–398. [PubMed: 15864268]

Myers JD. Growing old with HIV: the AIDS epidemic and an aging population. JAAPA. 2009; 22:20–24. [PubMed: 19248356]

Nottet HS, Persidsky Y, Sasseville VG, Nukuna AN, Bock P, Zhai QH, Sharer LR, McComb RD, Swindells S, Soderland C, Gendelman HE. Mechanisms for the transendothelial migration of HIV-1-infected monocytes into brain. J Immunol. 1996; 156:1284–1295. [PubMed: 8558009]

Onen NF, Overton ET, Seyfried W, Stumm ER, Snell M, Mondy K, Tebas P. Aging and HIV infection: a comparison between older HIV-infected persons and the general population. HIV Clin Trials. 2010; 11:100–109. [PubMed: 20542846]

Persidsky Y, Heilman D, Haorah J, Zelivyanskaya M, Persidsky R, Weber GA, Shimokawa H, Kaibuchi K, Ikezu T. Rho-mediated regulation of tight junctions during monocyte migration across the blood-brain barrier in HIV-1 encephalitis (HIVE). Blood. 2006; 107:4770–4780. [PubMed: 16478881]

Pu H, Tian J, Andras IE, Hayashi K, Flora G, Hennig B, Toborek M. HIV-1 Tat protein-induced alterations of ZO-1 expression are mediated by redox-regulated ERK 1/2 activation. J Cereb Blood Flow Metab. 2005; 25:1325–1335. [PubMed: 15829913]

Pu H, Tian J, Flora G, Lee YW, Nath A, Hennig B, Toborek M. HIV-1 Tat protein upregulates inflammatory mediators and induces monocyte invasion into the brain. Mol Cell Neurosci. 2003; 24:224–237. [PubMed: 14550782]

Pulliam L. HIV regulation of amyloid beta production. J Neuroimmune Pharmacol. 2009; 4:213–217. [PubMed: 19288202]

Ramirez SH, Heilman D, Morsey B, Potula R, Haorah J, Persidsky Y. Activation of peroxisome proliferator-activated receptor gamma (PPARgamma) suppresses Rho GTPases in human brain microvascular endothelial cells and inhibits adhesion and transendothelial migration of HIV-1 infected monocytes. J Immunol. 2008; 180:1854–1865. [PubMed: 18209083]

Rempel HC, Pulliam L. HIV-1 Tat inhibits neprilysin and elevates amyloid beta. AIDS. 2005; 19:127–135. [PubMed: 15668537]

Rosenberg GA. Matrix metalloproteinases and their multiple roles in neurodegenerative diseases. Lancet Neurol. 2009; 8:205–216. [PubMed: 19161911]

Shimada H, Rajagopalan LE. Rho kinase-2 activation in human endothelial cells drives lysophosphatidic acid-mediated expression of cell adhesion molecules via NF-kappaB p65. J Biol Chem. 2010; 285:12536–12542. [PubMed: 20164172]

Slotta JE, Braun OO, Menger MD, Thorlacius H. Fasudil, a Rho-kinase inhibitor, inhibits leukocyte adhesion in inflamed large blood vessels in vivo. Inflamm Res. 2006; 55:364–367. [PubMed: 17122957]

Thal DR, Griffin WS, de Vos RA, Ghebremedhin E. Cerebral amyloid angiopathy and its relationship to Alzheimer's disease. Acta Neuropathol. 2008; 115:599–609. [PubMed: 18369648]

Toborek M, Lee YW, Pu H, Malecki A, Flora G, Garrido R, Hennig B, Bauer HC, Nath A. HIV-Tat protein induces oxidative and inflammatory pathways in brain endothelium. J Neurochem. 2003; 84:169–179. [PubMed: 12485413]

Valcour V, Shikuma C, Shiramizu B, Watters M, Poff P, Selnes O, Holck P, Grove J, Sacktor N. Higher frequency of dementia in older HIV-1 individuals: the Hawaii Aging with HIV-1 Cohort. Neurology. 2004; 63:822–827. [PubMed: 15365130]

Weis S, Haug H, Budka H. Vascular changes in the cerebral cortex in HIV-1 infection: I. A morphometric investigation by light and electron microscopy. Clin Neuropathol. 1996; 15:361–366. [PubMed: 8937785]

Weksler BB, Subileau EA, Perriere N, Charneau P, Holloway K, Leveque M, Tricoire-Leignel H, Nicotra A, Bourdoulous S, Turowski P, Male DK, Roux F, Greenwood J, Romero IA, Couraud PO. Blood-brain barrier-specific properties of a human adult brain endothelial cell line. FASEB J. 2005; 19:1872–1874. [PubMed: 16141364]

Wennerberg K, Rossman KL, Der CJ. The Ras superfamily at a glance. J Cell Sci. 2005; 118:843–846. [PubMed: 15731001]

Yankner BA, Lu T, Loerch P. The aging brain. Annu Rev Pathol. 2008; 3:41–66. [PubMed: 18039130]

Yong VW, Power C, Forsyth P, Edwards DR. Metalloproteinases in biology and pathology of the nervous system. Nat Rev Neurosci. 2001; 2:502–511. [PubMed: 11433375]

Zhong Y, Hennig B, Toborek M. Intact lipid rafts regulate HIV-1 Tat protein-induced activation of the Rho signaling and upregulation of P-glycoprotein in brain endothelial cells. J Cereb Blood Flow Metab. 2009; 30:522–533. [PubMed: 19794400]

Zhong Y, Smart EJ, Weksler B, Couraud PO, Hennig B, Toborek M. Caveolin-1 regulates human immunodeficiency virus-1 Tat-induced alterations of tight junction protein expression via modulation of the Ras signaling. J Neurosci. 2008; 28:7788–7796. [PubMed: 18667611]

Zipfel GJ, Han H, Ford AL, Lee JM. Cerebral amyloid angiopathy: progressive disruption of the neurovascular unit. Stroke. 2009; 40(3 Suppl):S16–19. [PubMed: 19064794]

Zlokovic BV. The blood-brain barrier in health and chronic neurodegenerative disorders. Neuron. 2008; 57:178–201. [PubMed: 18215617]
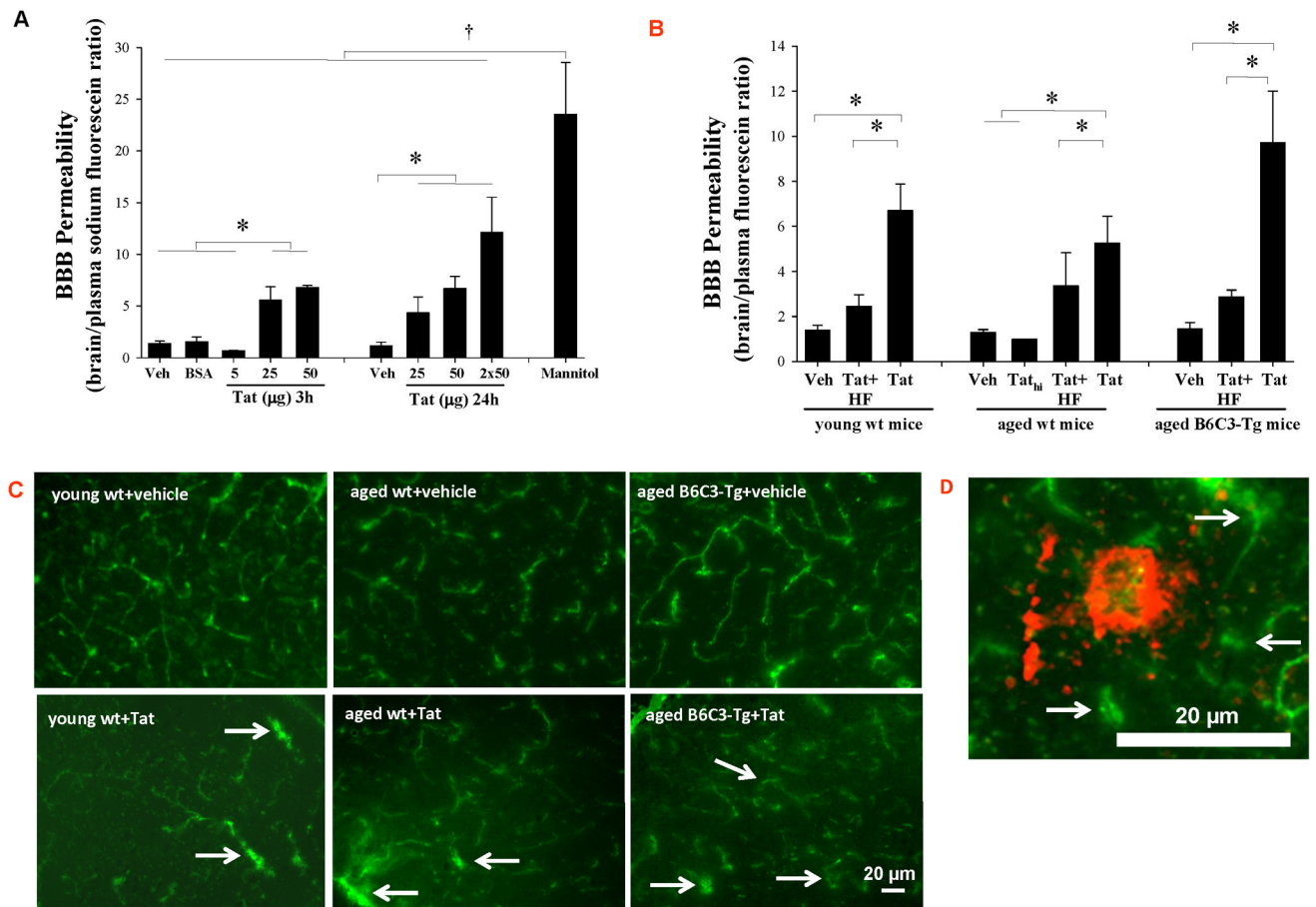
Figure 1. Brain Aβ deposits potentiate Tat-induced disruption of the BBB integrity
(A) Young (3 month old) C57BL/6 mice were injected with the indicated doses of Tat (5, 25, 50 µg), vehicle (Veh) or bovine serum albumin (BSA) into the internal carotid artery (ICA). The BBB integrity was evaluated 3 and 24 h post Tat administration by injecting 100 µl 2% sodium fluorescein (NaF) into the ICA. Fifteen minutes post NaF injection, permeability across the BBB was calculated as the ratio of fluorescence in the brain tissue to plasma. Mannitol (20% in PBS, 200 µl; 15 min exposure) was used as positive control. **(B)** Tat-induced disruption of the BBB integrity was compared in aged (12 month old) B6C3-Tg mice overexpressing Aβ, age-matched littermate wild type (wt) controls, and young (3 month old) wt C57BL/6 mice. Tat (25 µg) was administered as in (A) and heat-inactivated Tat (Tat$_{hi}$) was used as negative control. Selected groups of mice were also injected with hydroxyfasudil (HF; Rho inhibitor; 100 µM, i.p.) 12 h prior to Tat administration. Permeability across the BBB was assessed as in (A). **(C)** Integrity of the cerebral microvasculature as determined by leakage of FITC-albumin. Young and aged mice were injected with 25 µg Tat as in (A). Twenty four hours later, the animals were perfused with saline, followed by 4 ml 5% FITC-albumin. Control brains show normal staining pattern in which fluorescence is retained within the cerebral vessels. In contrast, the staining is diffused in the ipsilateral hemisphere of Tat-injected brains, indicating albumin leakage. Images shown are the representative data from 4 experiments; the arrows indicate albumin leakage. **(D)** A typical amyloid plaque in the brain of 12 month old B6C3-Tg mice. Vessel integrity was evaluated as in (C). An advanced amyloid plaque is surrounded by a diffused microvessel network with substantial capillary leakage (arrows), indicating compromised

BBB integrity. Data in A and B are mean ±SEM, n= 4–10 in each group; *, p< 0.05; †, p< 0.01. The scale bar, 20 µm.
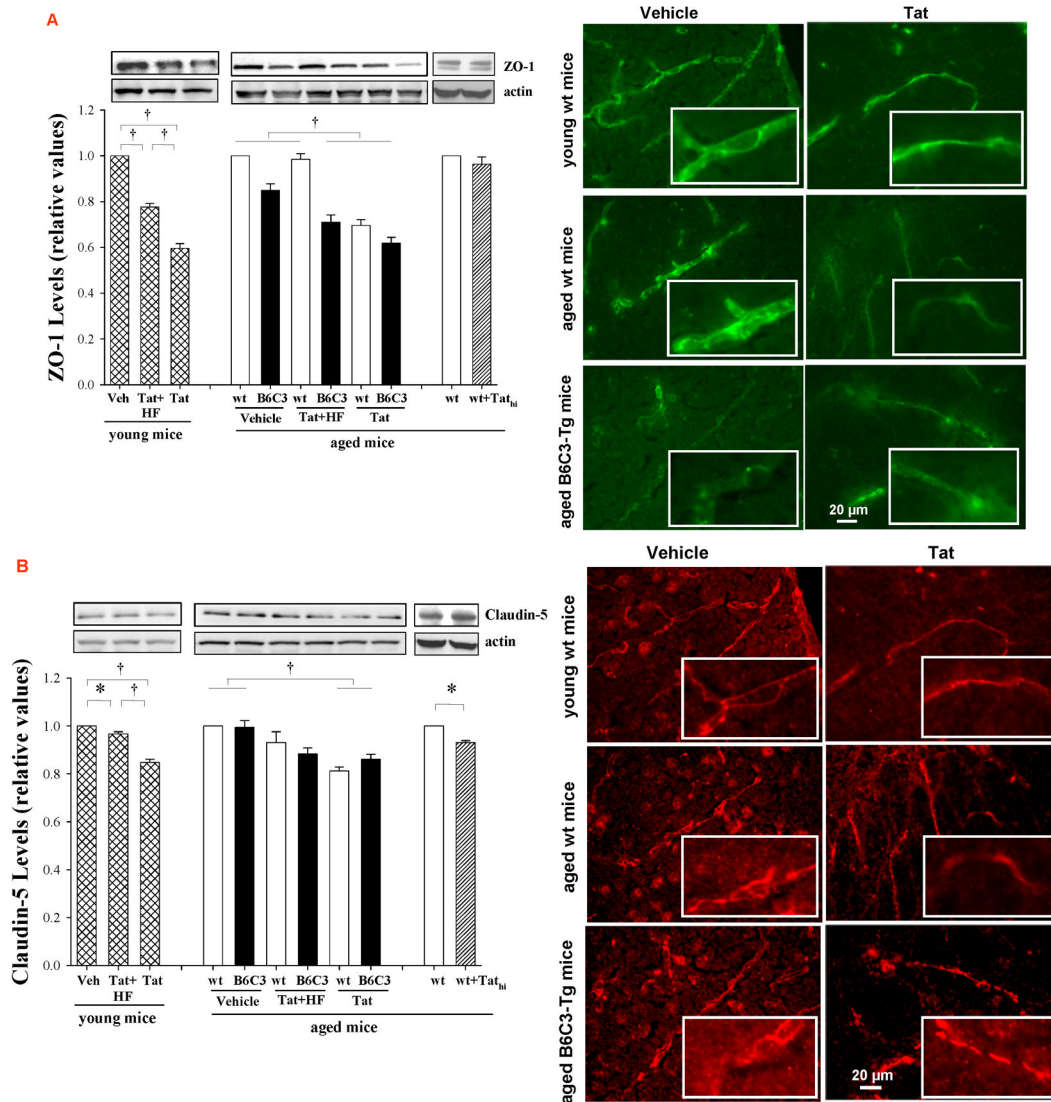
Figure 2. Tat-induced alterations of tight junction (TJ) protein expression in young and aged mice

Aged (12 month old) B6C3-Tg mice, age-matched littermate controls, and young (3 month old) C57BL/6 mice were injected with Tat, Tat_{hi}, or hydroxyfasudil (HF) as in Figure 1. Expression of ZO-1 (**A**) and claudin-5 (**B**) was analyzed 24 h post Tat administration by Western blotting (left panels) and fluorescent microscopy (right panels). In immunostaining studies, ZO-1 and claudin-5 revealed continuous and linear staining in the control mice. In contrast, immunoreactivity of these TJ proteins was decreased and exhibited a dotted and fragmented staining pattern in Tat-injected mice. Images were taken using a 40x lens and are representative from 4 experiments. Data in (A) are mean ±SEM, n= 4–7 in each groups; *, p< 0.05; †, p< 0.01.
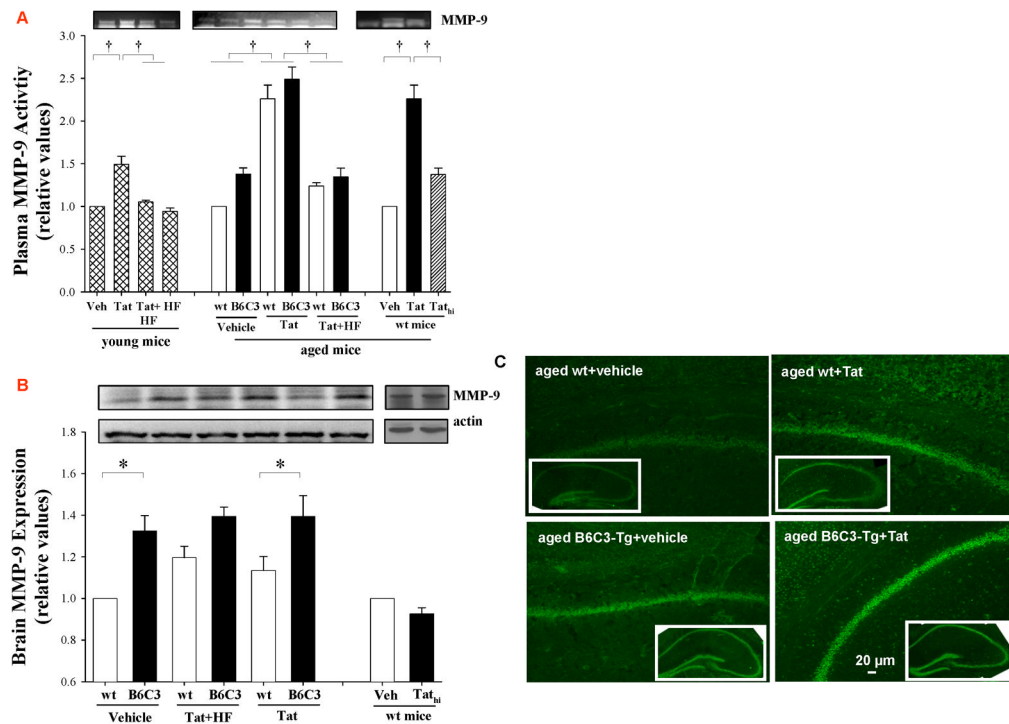
Figure 3. Tat-induced MMP-9 expression is potentiated in B6C3-Tg mice
Mice were injected with Tat, Tat$_{hi}$, or hydroxyfasudil (HF) as in Figure 1 and analyses were performed 24 h post Tat injection. **(A)** Plasma MMP-9 activity was determined by zymography. **(B)** Expression of MMP-9 protein in the brain tissue was assessed by Western blotting. Data are mean ±SEM, n= 4–5; *, p< 0.05; †, p< 0.01. **(C)** *In situ* zymography was performed to visualize gelatinase activity in the hippocampal sections of aged B6C3-Tg and control mice. Images are representative from 4 experiments.
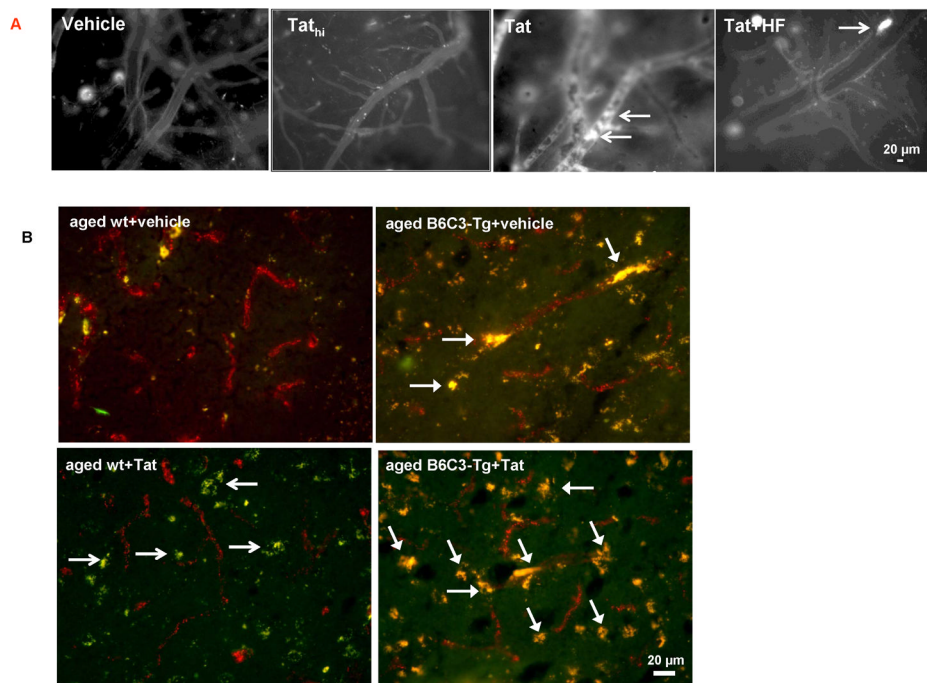
Figure 4. Exposure to Tat induces leukocyte attachment to the brain endothelium and the presence of inflammatory cells in brain parenchyma
(A) Young (3 month old) mice were operated to install cranial window, followed by injection with Tat, Tat$_{hi}$, or hydroxyfasudil (HF), as in Figure 1. Circulatory leukocytes were labeled with rhodamine 6G and the interaction of labeled leukocytes with cerebral vessels was visualized 3 h post Tat injection via the cranial window under a confocal microscope. Arrows indicate leukocytes attached to the brain endothelium. Images are representative from 4 experiments. **(B)** Aged B6C3-Tg and age-matched wild type control mice were exposed to Tat for 24 h as in Figure 1. Brain slices were stained for factor VIII (endothelial cell marker, red staining) and for F4/80 antigen (macrophage marker, green staining). The areas of colocalization of endothelial cells with macrophages are depicted in yellow.
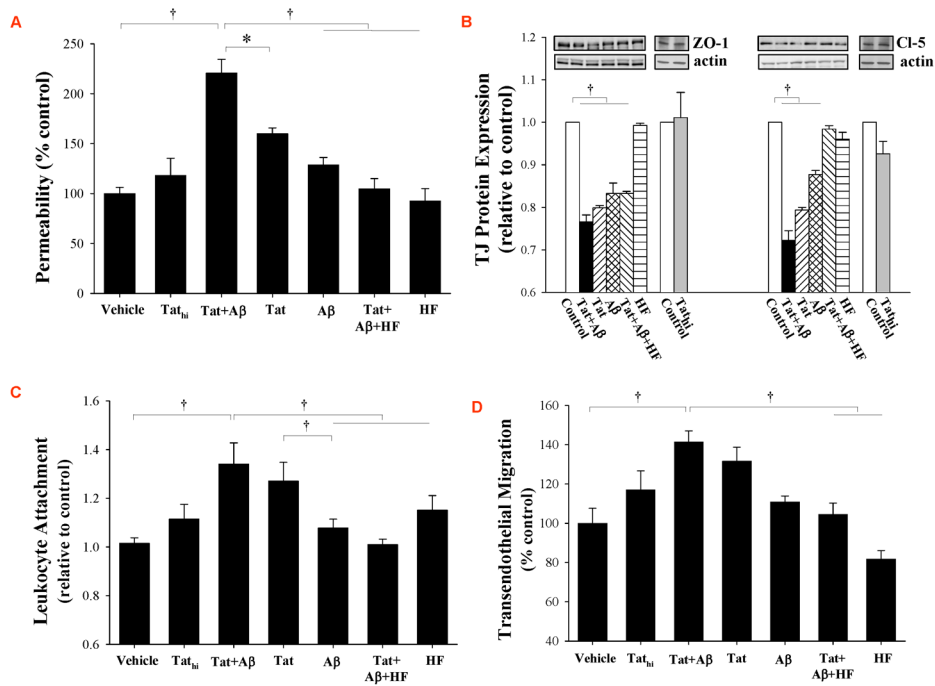
Figure 5. Aβ potentiates Tat-induced toxicity in brain endothelial cells
(A) Confluent HCMEC/D3 cells were serum deprived for 12 h, followed by treatment with Tat (100 nM), Tat$_{hi}$, and/or Aβ (1 µM) for 24 h. Additional cultures were also exposed to Rho inhibitor hydroxyfasudil (HF, 100 µM, pretreatment for 12 h). Then, permeability was measured by transendothelial flux of FITC-dextran 20 kDa. **(B)** HCMEC/D3 cells were treated as in (A), followed by determination of ZO-1 and claudin-5 protein levels by Western blotting. **(C)** Confluent HCMEC/D3 cells were treated as in (A). Then, 1×10^4 fluorescently labeled THP-1 monocytic cells were added for 30 min to HCMEC/D3 cultures and the attachment was assessed using a fluorescence plate reader. **(D)** Confluent HCMEC/D3 cells cultured on Transwell inserts were treated as in (A). CCL-2 (50 ng/ml) was added to the lower chamber of the Transwell system. THP-1 monocytic cells were added into the upper chamber, and cell migration across HBMEC/D3 monolayers was measured 2 h later. Data are mean ±SEM, n=5–7; *, p< 0.05; †, p< 0.01.